2018

Sliding-mode and proportional-resonant based control strategy for three-phase two-leg T-type grid-connected inverters with LCL filter

Necmi Altin

Saban Ozdemir

Hasan Komurcugil

See next page for additional authors

Authors

Necmi Altin, Saban Ozdemir, Hasan Komurcugil, Ibrahim Sefa, and Samet Biricik

Sliding-Mode and Proportional-Resonant Based Control Strategy for Three-Phase Two-Leg T-Type Grid-Connected Inverters With LCL Filter

Necmi Altin[1], Saban Ozdemir[2], Hasan Komurcugil[3], Ibrahim Sefa[1]and Samet Biricik[4,5]
[1] Department of Electrical and Electronic Engineering, Faculty of Technology, Gazi University, Ankara, Turkey.
[2] Department of Energy Systems Engineering, Faculty of Technology, Gazi University, Ankara, Turkey.
[3] Department of Computer Engineering, Eastern Mediterranean University, Famagusta, Via Mersin 10, Turkey.
[4] Department of Electrical and *Electronics Eng.*, European University of Lefke, Lefke, Northern Cyprus TR-10 Mersin, Turkey
[5] School of Electrical & Electronic Engineering, Dublin Institute of Technology (DIT), Dublin, Ireland.
naltin@gazi.edu.tr, sabanozdemir@gazi.edu.tr, hasan.komurcugil@emu.edu.tr, isefa@gazi.edu.tr, sbiricik@eul.edu.tr

***Abstract*—In this study, sliding-mode and proportional-resonant based control strategy is proposed for three-phase two-leg T-type grid-connected inverter with LCL filter. The sliding surface function is formed by using the inverter current and capacitor voltage errors. When the inverter current and capacitor voltage feedbacks are included into the control loop, the active damping requirement is automatically resolved. The PR controllers are employed in cascaded manner to generate the references for inverter current and capacitor voltage. The use of PR controllers ensures zero steady-state error in the inverter current, capacitor voltage and grid current. In addition, since the proposed three-phase inverter has only two legs, the total switch count is reduced resulting in cheaper and reliable topology. The proposed system is validated through computer simulations which show that proposed control algorithm can achieve the control of grid currents. The total harmonic distortion level of the grid currents is in the limits of international standards.**

Keywords—Reduced number of switches, two-leg, SMC, proportional resonant, grid interactive.

I. INTRODUCTION

The interest on renewable energy resources is increasing to obtain clean, sustainable, secure energy sources. As a result of these studies, solar and wind energy conversion systems have become more popular because of repetitive cost of wind power conversion systems, and modular nature from a few watts to megawatts and wide installment capacity of photovoltaic systems. In addition, these resources contribute to distributed energy generation systems. Generally, the specification of the energy required by the consumer devices is incompatible with energy produced by renewable resources. It is necessary to adapt the electrical energy generated by renewable resources via converters and/or inverters. Since, generally loads are supplied with the AC energy, grid-connected or stand-alone (local) inverters are used for this purpose [1].

Although voltage source inverters (VSI) and current source inverter (CSI) can be used in grid-connected inverter applications. The VSIs are more common with easy control features. However, increasing desired power and voltage levels and tendency on high efficiency increase the usage of the multi-level inverters. As the number of levels increases, the output quality improves. Multi-level inverters offer advantages such as low filter requirement, low EMI level, high efficiency, allowing ordinary semiconductor switches to be used in higher voltage level applications and to access higher power level with these ordinary switches. As a result, three-level inverters are often preferred for medium and high power applications. However, there are some disadvantages. These can be listed as having a more complex structure, increasing number of semiconductor switches and driver requirement which increases the cost and size. The cascaded H-bridge, flying capacitor and neutral point clamped inverters are the most common multi-level inverter topologies. Each of these topologies has their own advantages and disadvantages. The NPC inverter removes the isolated power source as well as large capacitor requirements, but it suffers from the voltage and power loss unbalance problems [2-4]. Different control schemes and modified topologies have been proposed to resolve these drawbacks [5, 6]. The T-type inverter is emerged as one of these topologies. Compared to the conventional NPC inverters, there is no clamping diode requirement in the T-type inverters [7].

Many studies have been investigated on multi-level inverters to achieve more compact and more efficient inverter topology with reduced number of switch [8]. The nine-level inverter has been proposed with 10 semiconductor switches and 4 clamping diodes [9]. However, this topology also requires coupled-inductors. The n-level inverter topology (tested as 53-level) [10] and the multiple-poles multi-level diode-clamped inverter [11] with reduced number of switches have been proposed. Although these studies provide significant reduction in number of switches, they require bi-directional switches. There is no proposed structure and control method for T-type inverter with reduced number of switches.

L, LCL and LLCL filters are proposed for grid-interactive inverter applications. The L filter is a first order filter. For the suppression of current harmonics, a very large filter is required [12]. As a result, size, weight and losses of the filter increase. Furthermore, the increase in voltage drop on L filter have a negative effect on the relation between DC bus and inverter output. It also causes an increase in losses [13]. The LLCL filter is also suggested single- or three-phase grid-connected inverters [14]. Significant improvements in filter performance have been reported with the LLCL filter. But, the high number of elements and increase in order is disadvantageous due to the difficulties in defining the system model and the difficulty of

978-1-5090-6684-1/18/$31.00 ©2018 IEEE

control. Compared to the L filter, the third-order LCL filter offers better harmonic suppression as well as smaller size, weight and lower cost. However, the LCL filters have also cause oscillation and damping problems. This may requires extra damping precautions known in the literature as active damping and passive damping methods [15]. Although passive damping is a good method of suppression, the use of a resistor added to the filter results in a decrease in efficiency as well as a decrease in filtering features. It may be appropriate solution to define a virtual resistor in a closed loop system instead of a real resistor to remove these disadvantages. Active suppression methods are more preferred, although they require extra sensors and increase the complexity [16].

Control of grid-connected inverters with LCL filter is a hot topic in the literature. The resonance damping requirement is achieved by active damping methods which make use of inverter current [17], capacitor current [18], capacitor voltage [19], grid current [20] and two-current-loop [21]. In addition, the voltage-oriented proportional-integral (PI) controller is widely used in the synchronous rotating dq frame for regulating the d- and q-component currents of three-phase grid-tied VSI [22]-[24]. The sliding mode control (SMC) strategy provides fast dynamic response, robustness against parameter variations and disturbances and decreases the control complexity. Although it is applied for power converter applications, there is limited number of studies for three-phase grid-connected inverter with LCL filter [25], [26].

In this study, three-phase two-leg T-type inverter with LCL filter is proposed for grid-connected applications. When compared with the conventional one, the proposed inverter has only two inverter legs. Thus, the total size, volume and cost are reduced. The control algorithm is based on SMC and proportional resonant (PR) controllers which are used to generate inverter current and capacitor voltage references. Then, the sliding surface function in terms of the inverter current and capacitor voltage errors is formed. The double-band hysteresis based switching logic is used to generate the required PWM signals which lead to a reduction in the switching frequency. Simulation studies carried out via MATLAB/Simulink show that the proposed two-leg inverter generates sinusoidal currents and injects them to the grid. Also, the use of PR controllers guarantees that the inverter current, grid current and capacitor voltage can track their references with zero steady-state error. Moreover, employing the inverter current and capacitor voltage in the sliding surface function eliminates the need for using a dedicated active damping method. In addition, the proposed system meets the international standards such as IEEE1547 and IEC61727 in terms of power quality indices.

II. Three-Phase Two-Leg T-Type Grid-Connected Inverter Modeling

First reduced switch count inverters have been proposed for motor drive and electrical vehicle applications. These structures were based on a two-level inverter topology. In these topologies, the three-phase voltage can be obtained with two inverter legs instead of three inverter legs. The three-phase conventional inverter (which is also called B6 inverter) and three-phase two-leg inverter (which is also called B4 inverter) are depicted in Fig. 1. These inverters can operate with two-thirds of the switches and drives. Thus, they are the focus of researchers because they contain fewer switches and drives than ordinary inverters. They applied to different applications such as STATCOM, active power filter, three-level inverters and stand-alone and grid-connected inverters. [27-34].

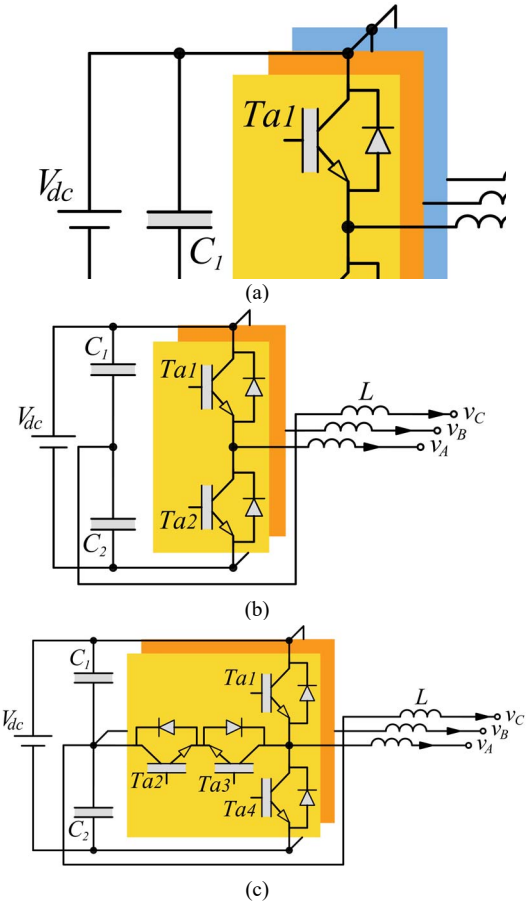

Fig. 1. Inverter topologies a) Three-phase VSI, b) Three-phase four-switch inverter, c) Three-phase three-level T-type inverter

Three-phase two-leg T-type grid-connected inverter with an LCL filter is shown in Fig. 2. It is seen that there are two switch-legs for phases a and b. The third phase is directly connected to the DC bus midpoint. Total number of active switches is 8; while these are 12 for conventional three-phase three-level T-type inverter. The operation of the system under balanced grid can be described by the following equations

$$L_1 \frac{di_{1a}}{dt} + r_1 i_{1a} = \frac{2}{3} u_a V_{dc} - \frac{1}{3} u_b V_{dc} - v_{Ca} \quad (1)$$

$$L_1 \frac{di_{1b}}{dt} + r_1 i_{1b} = \frac{2}{3} u_b V_{dc} - \frac{1}{3} u_a V_{dc} - v_{Cb} \quad (2)$$

$$L_1 \frac{di_{1c}}{dt} + r_1 i_{1c} = -\frac{1}{3} u_a V_{dc} - \frac{1}{3} u_b V_{dc} - v_{Cc} \quad (3)$$

$$L_2 \frac{di_{2k}}{dt} + r_2 i_{2k} = v_{Ck} - v_{gk} \quad (4)$$

$$C\frac{dv_{ck}}{dt} = i_{1k} - i_{2k} \tag{5}$$

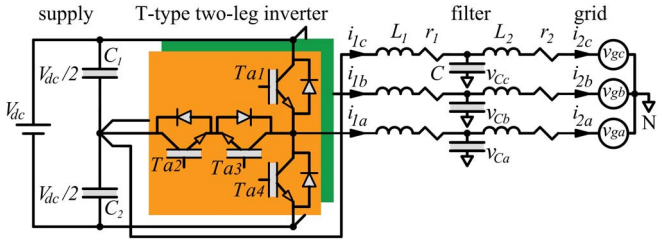

Fig. 2. Three-phase two-leg T-type grid-connected inverter with an LCL filter.

where $k = a,b$, $v_{gk} = V_g \cos(\omega t + \phi)$ is the grid voltage with ϕ taking 0, $-2\pi/3$, and $-4\pi/3$ for phases A, B and C, respectively and the control signal is given as

$$u_k = \frac{1}{4}(T_{1k} + T_{2k} - T_{3k} - T_{4k}) \tag{6}$$

The current injected into the grid is required to be sinusoidal with low THD. Therefore, the reference for i_{2k} can be defined as

$$i_{2k}^* = I_2^* \cos(\omega t + \phi) \tag{7}$$

where I_2^* is the desired amplitude of i_{2k}^*.

III. Sliding Mode Control Strategy

As mentioned in Introduction, the resonance damping is essential in grid-connected LCL-filtered inverter systems. In [15] and [16], the sliding surface function is formed by using the capacitor voltage error and its derivative. In [14], it is shown that the inclusion of capacitor voltage feedback in the control loop has a natural damping effect. Therefore, the damping issue can be tackled automatically by using the capacitor voltage feedback in the sliding surface function without using a dedicated active damping method. However, the derivative requirement in these control methods is the major drawback. Unlike the sliding surface functions defined in [15] and [16], the sliding surface function in this study is defined as

$$S_k = k_1 x_{1k} + k_2 x_{2k} \tag{8}$$

where k_1 and k_2 are positive real constants, x_{1k} and x_{2k} denote the state variables defined as

$$x_{1k} = v_{ck} - v_{ck}^* \tag{9}$$

$$x_{2k} = i_{1k} - i_{1k}^* \tag{10}$$

In (9) and (10), v_{ck}^* and i_{1k}^* are the references for v_{ck} and i_{1k}, respectively. It is well known that when the system enters into the sliding mode ($S_k = 0$), the state variables are forced to move on the sliding surface towards the origin ($x_{1k} = 0$ and $x_{2k} = 0$). In order to maintain the movement of the state variables on the sliding surface, the following condition must be satisfied

$$S_k \dot{S}_k < 0 \tag{11}$$

where $\dot{S}_k$ denotes the time derivative of S_k. The time derivative of (8) can be written as

$$\dot{S}_k = k_1 \dot{x}_{1k} + k_2 \dot{x}_{2k} \tag{12}$$

The PWM signals can be generated by using the double band hysteresis control (DBHC) proposed in [16] as follows

In the positive cycle of $S_k \Rightarrow T_{k1} = 0$ and $T_{k3} = 1$

$$T_{k2} = \begin{cases} 0 & \text{when} \quad S_k > +h \\ 1 & \text{when} \quad S_k < 0 \end{cases}, \quad T_{k4} = \begin{cases} 1 & \text{when} \quad S_k > +h \\ 0 & \text{when} \quad S_k < 0 \end{cases} \tag{13}$$

In the negative cycle of $S_k \Rightarrow T_{k2} = 1$ and $T_{k4} = 0$

$$T_{k1} = \begin{cases} 0 & \text{when} \quad S_k > 0 \\ 1 & \text{when} \quad S_k < -h \end{cases}, \quad T_{k3} = \begin{cases} 1 & \text{when} \quad S_k > 0 \\ 0 & \text{when} \quad S_k < -h \end{cases} \tag{14}$$

where h denotes the hysteresis band. The main advantage of this switching logic is that only two switching devices on each inverter leg are switched during the fundamental half-cycle while other two remain on or off in the other half-cycle. In [16], it is analytically shown that such switching reduces the switching frequency of the inverter.

IV. Reference Function Generation Using Cascaded PR Controllers

It is obvious from (9) and (10) that the reference functions v_{ck}^* and i_{1k}^* should be generated. Using (4) we obtain

$$v_{ck} = L_2 \frac{di_{2k}}{dt} + r_2 i_{2k} + v_{gk} \tag{15}$$

Hence, the reference of v_{ck} can be obtained by replacing i_{2k} with i_{2k}^* in (15) as follows

$$v_{ck}^* = L_2 \frac{di_{2k}^*}{dt} + r_2 i_{2k}^* + v_{gk} \tag{16}$$

Similarly, the equation for i_{1k}^* can be written with the help of (5) as follows

$$i_{1k}^* = C\frac{dv_{ck}^*}{dt} + i_{2k}^* \tag{17}$$

It is obvious from (16) and (17) that the generation of v_{ck}^* and i_{1k}^* requires measurement of the grid voltages, derivative operations and exact values of filter parameters like L_2, r_2 and C. However, it is not possible to estimate the exact values of the filter parameters as they are subject to change due to environmental and aging conditions. Proportional resonant (PR) controllers are able to track the AC quantities with zero steady-state error. Therefore, the PR controllers are commonly

used in inverter and rectifier control systems. In this study, the PR controllers are employed to generate v_{ck}^{*} and i_{1k}^{*}.

The AC signal tracking ability of the PR controller can be used to generate i_{1k}^{*}. When the grid current error $(i_{2k}^{*}-i_{2k})$ is applied to the PR controller, the output is i_{1k}^{*} such that i_{2k} tracks i_{2k}^{*} with zero steady-state error. The transfer function of PR controller is given by [35]

$$G_{PR}(s)=K_p+\frac{2K_r\omega_c s}{s^2+2\omega_c s+\omega^2} \tag{18}$$

where K_p and K_r are proportional and resonant gains, and ω_c is the cut-off frequency. The output of PR controller can be expressed in the Laplace domain as follows

$$I_{1k}^{*}(s)=\left(I_{2k}^{*}(s)-I_{2k}(s)\right)\frac{K_p^i s^2+2\omega_c\left(K_p^i+K_r^i\right)s+K_p^i\omega^2}{s^2+2\omega_c s+\omega^2} \tag{19}$$

where $I_{1k}^{*}(s)$, $I_{2k}^{*}(s)$, and $I_{2k}(s)$ denote the Laplace transforms of i_{1k}^{*}, i_{2k}^{*}, and i_{2k}, respectively.

Another PR controller can be used to generate v_{ck}^{*} by processing the inverter current error $(i_{1k}^{*}-i_{1k})$. Since the input of second PR controller involves i_{1k}^{*} which is the output of the first PR controller, it means that the PR controllers are connected in cascade manner as shown in Fig. 3.

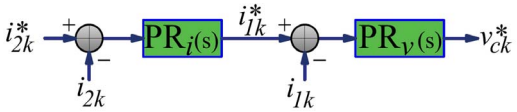

Fig. 3. Reference function generation with cascaded PR controllers.

In this case, i_{1k} tracks its reference i_{1k}^{*} with zero steady-state error. By using the transfer function given in (25), v_{ck}^{*} can be expressed in the Laplace domain as follows

$$V_{ck}^{*}(s)=\left(I_{1k}^{*}(s)-I_{1k}(s)\right)\frac{K_p^v s^2+2\omega_c\left(K_p^v+K_r^v\right)s+K_p^v\omega^2}{s^2+2\omega_c s+\omega^2} \tag{20}$$

where $V_{ck}^{*}(s)$, $I_{1k}^{*}(s)$, and $I_{1k}(s)$ denote the Laplace transforms of v_{ck}^{*}, i_{1k}^{*}, and i_{1k}, respectively.

V. Simulation Results

The proposed SMC technique using cascaded PR controllers has been tested by MATLAB/Simulink simulations. The block diagram of three-phase two-leg T-type grid-connected LCL-filtered inverter with the proposed control scheme is shown in Fig. 4. The system parameters are $V_g=230\sqrt{2}\,\mathrm{V}$, $L_1=1.7\,\mathrm{mH}$, $C=10\,\mu F$, $L_2=0.8\,\mathrm{mH}$, $r_1=0.17\,\Omega$, $r_2=0.076\,\Omega$, $V_{dc}=1200\,\mathrm{V}$, and $f=50\,\mathrm{Hz}$.

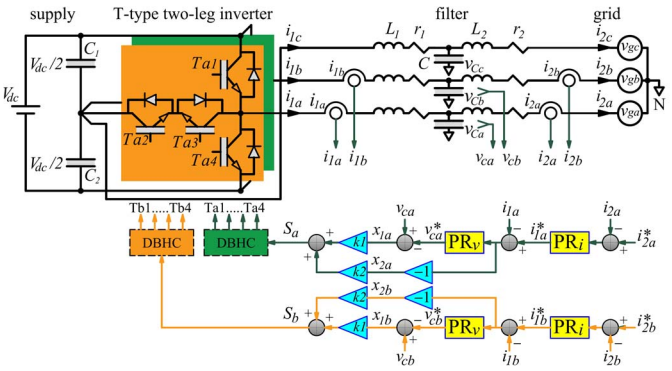

Fig. 4. Block diagram of three-phase two-leg T-type grid-connected LCL-filtered inverter with proposed control scheme.

The control parameters were selected as $K_1=5000$, $K_2=25000$, $h=22000$, $K_p^i=2.4$, $K_p^v=8$, $K_r^v=1250$, $K_r^v=7500$ and $\omega_c=1\,\mathrm{rad/s}$.

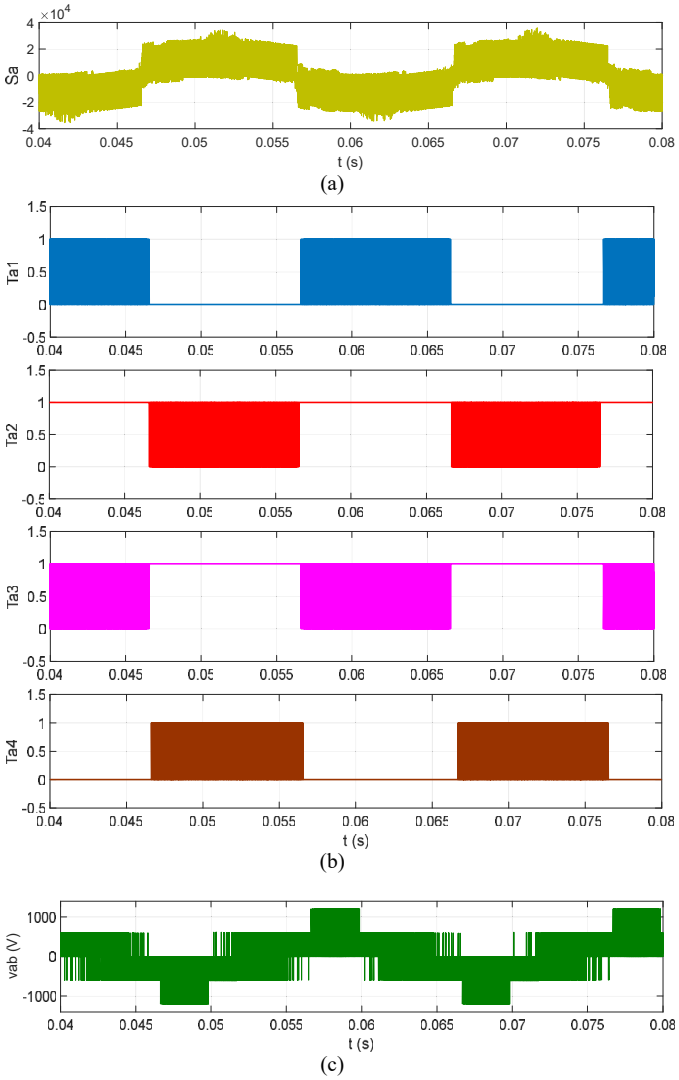

Fig. 5. Steady-state responses of phase-A: a) S_a, b) Switching signals (T_{a1}, T_{a2}, T_{a3}, T_{a4}) c) v_{ab}.

Fig. 5 shows the steady-state responses of phase-A sliding surface function, switching signals and phase-to-phase voltage at the output of inverter. It can be seen that S_a moves between the hysteresis bands (0, +22000) and (0, -22000) during a complete cycle. The double-band approach causes two switching devices on each inverter leg are switched during the fundamental half-cycle while other two remain on or off in the other half-cycle. Clearly, T_{a1} and T_{a3} are switched in complementary manner. Similarly, T_{a2} and T_{a4} are turned on and off in complementary manner. On the other hand, notice that the phase-to-phase voltage (v_{ab}) has five levels.

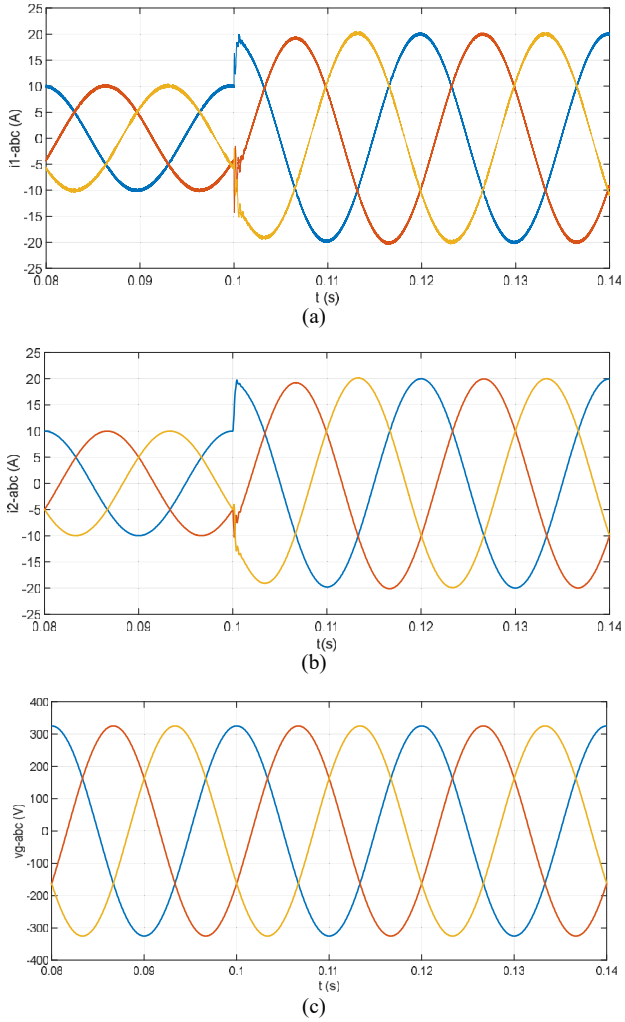

Fig. 6. Transient responses of the inverter variables for a step change in I_2^* from 10A to 20A; a) i_{1k} , b) i_{2k} and c) v_{gk} .

Fig. 6 shows the transient responses of three-phase inverter currents, grid currents and grid voltages for a step change in I_2^* from 10A to 20A at t=0.1s. It can be seen that the inverter injects balanced and sinusoidal currents to the grid. In addition, the grid currents are in phase with the grid voltages satisfying the unity power factor operation. The THD values of the grid currents are computed to be 1.3% and 0.86% for 10A and 20A operation conditions, respectively. It is worth noting that these values are below the limits defined by international standards.

Fig. 7 shows the start-up responses of phase-A inverter current, grid current and capacitor voltage together with their references. It can be easily seen that the actual waveforms track their references very fast and hence the actual waveforms overlap with their corresponding references. In such a case, no steady-state error exists.

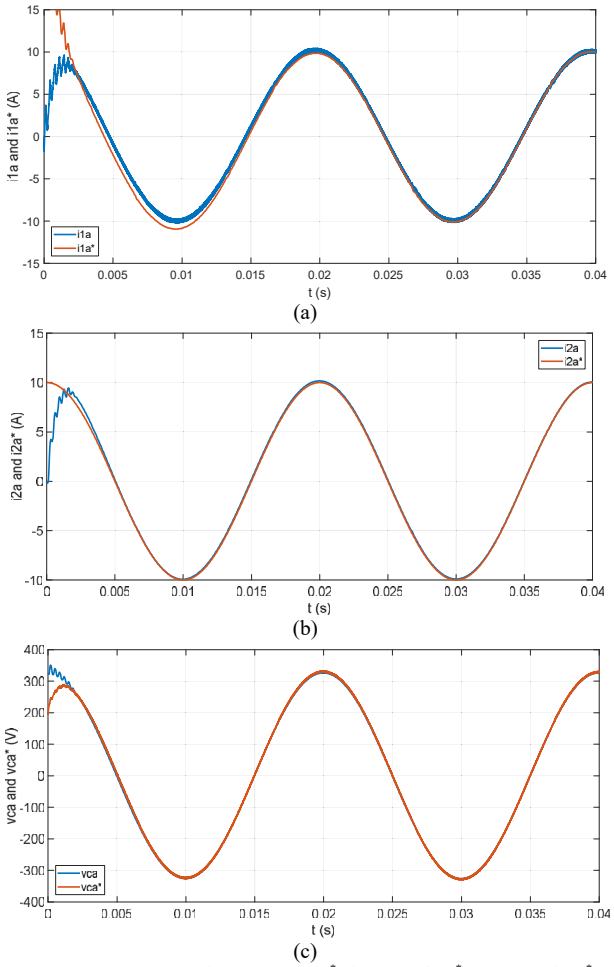

Fig. 7. Start-up responses of : a) i_{1a} and i_{1a}^* , b) i_{2a} and i_{2a}^* , a) v_{ca} and v_{ca}^* .

VI. CONCLUSIONS

In this study, a SMC and PR based control strategy is proposed for three-phase two-leg T-type grid-connected inverter with LCL filter. The SMC which employs the inverter current and capacitor voltage errors eliminates the active damping requirement. The use of PR controller eliminates the steady-state error in the grid current. The two-leg inverter topology reduces the switch count. The feasibility and performance of the proposed control scheme is validated through simulation studies. It is seen that the proposed control strategy works on the proposed two-leg inverter topology successfully and injects three-phase balanced currents to the grid with good steady-state (zero steady-state error and low THD in grid current) and fast transient response. Hence, with proposed inverter topology, one third reduction can be obtained in the total switch count.

REFERENCES

[1] R. K. Surapaneni and P. Das, "A Z-source-derived coupled-inductor-based high voltage gain microinverter," *IEEE Trans. Ind. Electron.*, vol. 65, no. 6, pp. 5114–5124, 2018.

[2] S. Ozdemir, N. Altin, and I. Sefa, "Single stage three level grid interactive MPPT inverter for PV systems," *Energy Convers. Manag.*, vol. 80, pp. 561–572, 2014.

[3] M. Schweizer and J. W. Kolar, "Design and implementation of a highly efficient three-level T-type converter for low-voltage applications," *IEEE Trans. Power Electron.,* vol. 28, pp. 899–907, 2013.

[4] N. Altin, and S. Ozdemir, "Three-phase three-level grid interactive inverter with fuzzy logic based maximum power point tracking controller," *Energy Convers. Manag.*, vol. 69, pp. 17–26, 2013.

[5] I. Lopez, S. Ceballos, J. Pou, J. Zaragoza, J. Andreu, E. Ibarra, and G. Konstantinou, "Generalized PWM-based method for multiphase neutral-point-clamped converters with capacitor voltage balance capability," *IEEE Trans. Power Electron.*, vol. 32, no. 6, pp. 4878–4890, June 2017.

[6] U. M. Choi and F. Blaabjerg, "Asymmetric power device rating selection for even temperature distribution in NPC inverter," *IEEE Energy Conversion Congress and Exposition* (ECCE), pp. 4196–4201, 2017.

[7] S. Ozdemir, "Z-source T-type inverter for renewable energy systems with proportional resonant controller," *International Journal of Hydrogen Energy*, vol. 41, no. 29, pp.12591–12602, 2016.

[8] M. Norambuena, S. Kouro, S. Dieckerhoff and J. Rodriguez, "Reduced multilevel converter: A novel multilevel converter with a reduced number of active switches," *IEEE Trans. Ind. Electron.,* vol. 65, no. 5, pp. 3636–3645, 2018.

[9] P. Chamarthi and A. Vivek, "A new couple inductor based 9-level inverter with reduced number of switches for standalone grid connected solar PV systems," *IEEE 40th Photovoltaic Specialist Conference (PVSC),* pp. 3094–3099, 2014.

[10] E. Babaei, "A cascade multilevel converter topology with reduced number of switches," *IEEE Trans. Power Electron*, vol. 23, no. 6, pp. 2657–266, 2008.

[11] O. H. P. Gabriel, A. I. Maswood, and A. Venkataraman, "Multiple-poles multilevel diode-clamped inverter (M2DCI) topology for alternative multilevel converter," *Conference on Power & Energy (IPEC)*, pp. 497–502, 2012.

[12] H. Komurcugil, N. Altin, S. Ozdemir, and I. Sefa, "Sliding-mode and proportional-resonant based control strategy for three-phase grid-connected LCL-filtered VSI," *IECON 2016 - 42nd Annual Conference of the IEEE Industrial Electronics Society*, pp. 2396–2401, 2016.

[13] H. Azani, A. Massoud, L. Benbrahim, B.W. Williams and D. Holiday, "An active damping approach for PR-based current control of grid-tied VSI with LCL filter," *8th IET International Conference on Power Electronics, Machines and Drives (PEMD 2016),* pp. 1–5, 2016.

[14] W. Wu, Y. He, T. Tang, and F. Blaabjerg, "A new design method for the passive damped LCL and LLCL filter-based single-phase grid-tied inverter," *IEEE Trans. Ind. Electron.*, vol. 60, no. 10, pp. 4339–4350, 2013.

[15] X. Li, J. Fang, Y. Tang, X. Wu and Y. Geng, "Capacitor-voltage feedforward with full delay compensation to improve weak grids adaptability of LCL-filtered grid-connected converters for distributed generation systems," *IEEE Trans. Power Electron.*, vol. 33, no. 1, pp. 749–764, 2018.

[16] H. Komurcugil, S. Ozdemir, I. Sefa, N. Altin, and O. Kukrer, "Sliding-mode control for single-phase grid-connected LCL-filtered VSI with double-band hysteresis scheme," *IEEE Trans. Ind. Electron.*, vol. 63, no. 2, pp. 864–873, 2016.

[17] E. Twining and D. G. Holmes, "Grid current regulation of a three-phase voltage source inverter with an LCL input filter," *IEEE Trans. Power Electron.*, vol. 18, no. 3, pp. 888–895, May 2003.

[18] W. Li, X. Ruan, D. Pan, and X. Wang, "Full-feedforward schemes of grid voltages for a three-phase LCL-type grid-connected inverter," *IEEE Trans. Ind. Electron.*, vol. 60, no. 6, pp. 2237–2250, Jun. 2013.

[19] I. J. Gabe, V. F. Montagner, and H. Pinherio, "Design and implementation of a robust current controller for VSI connected to the grid through an LCL-filter," *IEEE Trans. Power Electron.*, vol. 24, no. 6, pp. 1444–1452, Jun. 2009.

[20] J. Dannehl, C. Wessels, and F. W. Fuchs, "Limitations of voltage-oriented PI current control of grid-connected PWM rectifiers with LCL filters," *IEEE Trans. Ind. Electron.,* vol. 56, no. 2, pp. 380–388, Feb. 2009.

[21] F. Liu, Y. Zhou, S. Duan, J. Yin, B. Liu, and F. Liu, "Parameter design of a two-current-loop controller used in a grid-connected inverter system with LCL filter," *IEEE Trans. Ind. Electron.,* vol. 56, no. 11, pp. 4483-4491, Nov. 2009.

[22] A. Timbus, M. Liserre, R. Teodorescu, P. Rodriguez, and F. Blaabjerg, "Evaluation of current controllers for distributed power generation systems," *IEEE Trans. Power Electron.,* vol. 24, no. 3, pp. 654–664, March 2009.

[23] Q. Yan, X. Wu, X. Yuan, and Y. Geng, "An improved grid-voltage feedforward strategy for high-power three-phase grid-connected inverters based on the simplified repetitive predictor," *IEEE Trans. Power Electron.,* vol. 31, no. 5, pp. 3880–3897, May 2016.

[24] M. B. Said-Romdhane, M. W. Naouar, I. Slama-Belkhodja, and E. Monmasson, "Robust active damping methods for LCL filter based grid connected converters," *IEEE Trans. Power Electron.,* vol. 32, no. 9, pp. 6739–6750, Sept. 2017.

[25] J. Morales, L. G. de Vicuna, R. Guzman, M. Castilla, A. Momeneh, J. T. Martinez, "Sliding mode control of three-phase grid-connected voltage-source inverter with vector operation," *IEEE 41st Annual Conference of the Industrial Electronics Society (IECON'15),* pp. 1182–1187. Japan, 2015.

[26] R. Guzman, L. G. de Vicuna, J. Morales, M. Castilla, and J. Miret, "Model-based active damping control for three-phase voltage source inverters with LCL filter," *IEEE Trans. Power Electron.,* vol. 32, no. 7, pp. 5637–5650, July 2016.

[27] K. K. Gupta, A. Ranjan, P. Bhatnagar, L. K. Sahu and S. Jain, "Multilevel inverter topologies with reduced device count: A review," *IEEE Trans. Power Electron.,* vol. 31, no. 1, pp. 135–151, 2016.

[28] G. T. Kim and T. A. Lipo, "VSI-PWM rectifier/inverter system with a reduced switch count," *IEEE Trans. Ind. Appl.,* vol. 32, no. 6, pp. 1331–1337, 1996.

[29] I. Sefa, H. Komurcugil, S. Demirbas, N. Altin, and S. Ozdemir, "Three-phase three-level inverter with reduced number of switches for stand-alone PV systems renewable energy research and applications", *IEEE 6th International Conference on Renewable Energy Research and Applications (ICRERA),* pp. 1119–1124, 2017.

[30] M. S. Zaky and M. K. Metwaly, "A performance investigation of a four-switch three-phase inverter-fed IM drives at low speeds using fuzzy logic and PI controllers," *IEEE Trans. Power Electron.*, vol. 32, no. 5, pp. 3741–3753 , May. 2017.

[31] N. Altin, I. Sefa, H. Komurcugil, and S. Ozdemir, "Three-phase three-level T-type grid-connected inverter with reduced number of switches," *6th International Istanbul Smart Grids and Cities Congress and Fair (ICSG 2018),* pp. 58–62, April 2018.

[32] F. Blaabjerg, S. Freysson, H. H. Hansen, and S. Hansen, "A new optimized space-vector modulation strategy for a component-minimized voltage source inverter," *IEEE Trans. Power Electron.,* vol. 12, no. 4, pp. 704– 714, 1997.

[33] R. Agrawal, and S. Jain, "Comparison of reduced part count multilevel inverters (RPC-MLIs) for integration to the grid," *Electrical Power and Energy Systems*, vol. 84, pp. 214–224, 2017.

[34] W. U. K. Tareen and S. Mekhielf, "Three-phase transformerless shunt active power filter with reduced switch count for harmonic compensation in grid-connected applications," *IEEE Trans. Power Electron.*, vol. 33, no. 6, pp. 4868–4881, 2018.

[35] R. Teodorescu, F. Blaabjerg, M. Liserre, and P. Loh, "Proportional resonant controllers and filters for grid-connected voltage-source converters," *Proc. Inst. Electr. Eng.—Electr. Power Appl.*, vol. 153, no. 5, pp. 750–762, Sep. 2006.